Polymer 50 (2009) 1505–1515

Contents lists available at ScienceDirect

Polymer

journal homepage: www.elsevier.com/locate/polymer

Preparation and nonisothermal crystallization behavior of polypropylene/layered double hydroxide nanocomposites

Sunil P. Lonkar [a,b], S. Morlat-Therias [b], N. Caperaa [c], F. Leroux [c], J.L. Gardette [b], R.P. Singh [a,*]

[a] Division of Polymer Science and Engineering, National Chemical Laboratory, Pune 411 008, India
[b] Laboratoire de Photochimie Moléculaire et Macromoléculaire (UMR CNRS-UBP 6505), Université Blaise Pascal (Clermont II), 63170 Aubière, France
[c] Laboratoire des Matériaux Inorganiques (UMR CNRS-UBP 6002), Université Blaise Pascal (Clermont II), 63170 Aubière, France

ARTICLE INFO

Article history:
Received 3 October 2008
Received in revised form
29 December 2008
Accepted 12 January 2009
Available online 20 January 2009

Keywords:
Polypropylene nanocomposites
Layered double hydroxide
Nonisothermal crystallization kinetics

ABSTRACT

Polypropylene (PP)/layered double hydroxide (LDH) nanocomposites were prepared via melt intercalation using dodecyl sulfate anion modified LDH and maleated PP as compatibilizing agent. Evidently the interlayer anions in LDH galleries react with maleic anhydride groups of PP-g-MA and lead to a finer dispersion of individual LDH layers in the PP matrix. The nanostructure was characterized by XRD and TEM; the examinations confirmed the nanocomposite formation with exfoliated/intercalated layered double hydroxides well distributed in the PP matrix. The nonisothermal crystallization behavior of resulting nanocomposites was extensively studied using differential scanning calorimetry (DSC) technique at various cooling rates. In nonisothermal crystallization kinetics, the Ozawa approach failed to describe the crystallization behavior of nanocomposites, whereas the Avrami analysis and Jeziorny method well define the crystallization behavior of PP/LDH nanocomposite. Combined Avrami and Ozawa analysis (Liu model) also found useful. The results revealed that very small amounts of LDH (1%) could accelerate the crystallization process relative to the pure PP and increase in the crystallization rates was attributed to the nucleating effect of the nanoparticles. Polarized optical microscopy (POM) observations also support the DSC results. The effective crystallization activation energy was estimated as a function of the relative degree of crystallinity using the isoconversional analysis. Overall, results indicated that the LDH particles in nanometer size might act as nucleating agent and distinctly change the type of nucleation, growth and geometry of PP crystals.

1. Introduction

In recent years, polymer/layered crystal nanocomposites have been recognized as one of the most promising research fields in material chemistry. The scientific and technological interest for tailoring and modifying the polymer properties has been driving a very vivid research on the nano-structured materials and nanoparticulate fillers which significantly increase the properties of polymers using only small levels of additive, typically between 3 and 5% by weight, which are far below that normally required from conventional micron-sized fillers to achieve a similar effect. In this regard, most emphasis has been given to silicate layer nanocomposites, which after intercalation and exfoliation within the polymer structure, increase the mechanical properties, reduce the gas and vapor transmission, and even decrease in some cases the flammability [1–3]. So far, the majority of the research work has been focused on cationic clays, like the naturally occurring montmorillonite systems, while the layered double hydroxide (LDH) systems have been much less reported in the literature.

The LDHs are the class of anionic or hydrotalcite-like clays represented by the general formula $M^{II}_{1-x}M^{III}_{x}(OH)_2]^{x+}$. $[(A^{n-})^{x/n}.mH_2O]$ where M^{II} and M^{III} are divalent and trivalent metal cations, respectively, and A^- is the interlayer anion (Fig. 1) [4,5]. The basic reason for selecting LDH is their typical metal hydroxide-like chemistry and conventional clay-like layered crystalline structure. The former is helpful in the direct participation in the flame inhibition through endothermic decomposition and stable char formation [6]. On the other hand, they have a layered structure with aspect ratios similar or even higher than that observed for aluminosilicates [6,7], and it makes LDH suitable for polymer nanocomposite preparation. In recent years, polymer/LDH nanocomposites have attracted a great interest because they exhibit improved physical and performance properties in comparison to the pristine polymers and conventional composites ([5,8,9] and ref. therein). For example, the nano-scale dispersion of LDH into various polymer matrices such as polyethylene (PE) [10], polyamide

* Corresponding author. Tel.: +91 20 25902091; fax: +91 20 25902615.
E-mail address: rp.singh@ncl.res.in (R.P. Singh).

0032-3861/$ – see front matter © 2009 Elsevier Ltd. All rights reserved.
doi:10.1016/j.polymer.2009.01.031

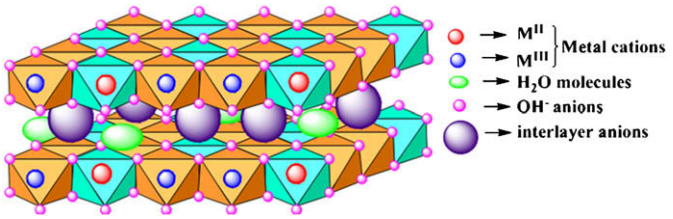

Fig. 1. Layered crystal structure of hydrotalcite-like compounds.

6 [11], epoxy [12], polystyrene [13], polyethylene terephthalate (PET) [14] polymethyl methacrylate (PMMA) [15], etc. has been reported. Polypropylene (PP) is one of the most widely used polyolefins has stimulated intensive research in order to produce polypropylene nanocomposites with enhanced properties. PP/LDH nanocomposites necessitate preparation and property investigation from the standpoint of commercial interest, therefore the study of the kinetics of crystallization is necessary for optimizing industrial process conditions and establishing the structure–property correlations in the polymer nanocomposites [16].

The study of the nonisothermal crystallization of polymers is of great technical importance, since most practical processing techniques proceed under nonisothermal conditions [17–19]. PP is semicrystalline polymer and the final properties of PP based composites in engineering applications are critically dependent on the extent of crystallinity which in turn depends on the processing conditions. The isothermal and nonisothermal crystallization kinetics of PP and its composites with different fillers have been extensively reported in the literature [20–30]. Xu et al. [20] studied the non-isothermal crystallization kinetics of PP/montmorillonite–clay nanocomposites and found that clay could accelerate the overall nonisothermal crystallization of PP and suggested a three-dimensional growth with heterogeneous nucleation for PP/clay nanocomposites. Maiti et al. [21] investigated how the crystallization controls the fine structure and morphology of the PP/clay nanocomposites. They concluded that the clay platelets act as a nucleating agent and lower the size of the PP spherulites. Qian et al. [22] successfully used models of Ozawa and Liu et al. to describe the nonisothermal crystallization of PP/nano SiO_2 composites and observed an increase of a few degrees of the crystallization temperature. He et al. [23] estimated an increase of 5 °C in the crystallization temperature of PP in the presence of nano-clay. The crystallization behavior of PP is also affected by carbon black [24], carbon nanotubes [25], graphite [26] and polyhedral oligomeric silsesquioxane [27]. Mucha et al. [24] reported that PP crystallization temperature increases by 8 °C with the addition of 5% carbon black. Grady et al. [25] reported a PP crystallization temperature increased by 5 °C with the addition of 1.8% carbon nanotubes while crystallization does not change under nonisothermal cooling conditions whereas Page et al. [26] studied crystallization behavior of PP/graphite nanocomposites and found that increase in crystallinity up to 20% and associated to a crystallization temperature shifted by 15 °C with the addition of 6–9% of graphite flakes.

Herein, for the first time the detailed investigation on the preparation of polypropylene and layered double hydroxide (LDH) type nanoparticles, organo-modified by surfactant molecules as filler and their effect on the nonisothermal crystallization behavior of PP in PP/LDH nanocomposites are scrutinized. To our knowledge, only few articles report the use of such inorganic/organic I/O LDH/surfactant assemblies as filler for polymers such as polyethylene-grafted-maleic anhydride, PE-g-MA [28] or poly(propylene carbonate) [29] but some are dealing with other polymers and their effect on the iso or nonisothermal crystallization behavior and the subsequent effect on changes of the microstructural parameters such as for poly(3-hydroxybutyrate) [30,31] and poly(ethylene terephthalate) PET [32]. The study focuses here on the preparation of PP/LDH nanocomposites by melt intercalation using PP-g-MA as a compatibilizer and their nonisothermal crystallization behavior. It is believed that the maleic anhydride groups can react with the interlayer anionic groups of LDH. The fine dispersion of LDH nanolayers and their interactions in polypropylene matrices have been characterized by FTIR, TEM and WAXD. The nonisothermal crystallization kinetics was achieved by confronting different models, namely Ozawa, Avrami and Liu et al. The spherulitic growth rate and the effective energy barrier of nonisothermal crystallization were explained by an isoconversional approach.

2. Experimental section

2.1. Materials

The isotactic polypropylene used in this study is Exxon Mobile PP with 2.5–3.5 MFI. The maleic anhydride-grafted-PP polymer (PP-g-MA) used as compatibilizer was a low molecular weight Polybond 3200 (MA content 1%, density – 0.91 g/cc and Mw – 90,000) obtained from Chemtura corporation. $MgCl_2 \cdot 6H_2O$ (Aldrich), $AlCl_3 \cdot 6H_2O$ (Aldrich), NaOH (Aldrich) and $C_{12}H_{25}O_4SNa$ (DDS, dodecyl sulfate – Sigma) were used as received.

2.2. Preparation of organo-modified Mg_2Al LDH

Hydrotalcite-type material Mg_2Al–DDS was prepared from anion exchange reaction. Chlorine Mg_2Al LDH phase was prepared by coprecipitation. Experimentally, the addition of metallic salts was performed at constant pH of 9 under nitrogen, this to avoid contamination by carbonate. The resulting powder was washed several times with decarbonated water, dried under vacuum. DDS was solubilized in a 400 mL decarbonated aqueous solution at 40 °C, and then Mg_2Al–Cl was added. The relative amount of DDS against Mg_2Al–Cl was an excess of 4 in DDS in comparison to the anion exchange capacity of the chlorine pristine LDH phase. The anion exchange reaction was let 48 h under nitrogen and vigorous stirring. The resulting powder was washed several times with a mixture EtOH/H_2O (50/50), and then dried under vacuum.

2.3. Nanocomposite preparation

Nanocomposites containing 1, 3 and 5% LDH nanoparticles were prepared by melt mixing in two steps using a co-rotating tightly intermeshed twin-screw extruder (DSM micro-compounder). All materials were dried at 80 °C under vacuum prior to mixing.

2.3.1. Step 1. Preparation of compatibilized PP

Isotactic polypropylene was mixed with MA-g-PP in a weight proportion of 95:5. The operation temperature was maintained at 180 °C for 5 min at 200 rpm rotor speed to prepare a master batch of compatibilizer in PP. All experiments were performed under inert atmosphere.

2.3.2. Step 2. Preparation of composites

The designated amount of Mg_2Al–DDS LDH was added to the molten compatibilized PP and mixed at 180 °C for 5 min keeping other parameters as above. The samples were abbreviated as PPL1, PPL3 and PPL5 for 1, 3 and 5% loading in PP, respectively.

The films of thickness between 80 and 100 μm were obtained using laboratory press at 180° under 4 tonnes of pressure for 2 min.

2.4. Microstructure characterization

2.4.1. FTIR analysis

The filler–polymer interactions were analyzed by FTIR. Infrared spectra were recorded using a Nicolet 5SX-FTIR spectrometer working with OMNIC software. Spectra were obtained using 32 scans and 4 cm^{-1} resolution. The spectra presented were baseline corrected and converted to the absorbance mode.

2.4.2. XRD characterization

The degree of swelling and the interlayer distance in layer structure of Mg_2Al–DDS LDH in the nanocomposites were determined by WAXD with Rigaku (Japan) D/max-RB wide angle X-ray diffractometer (WAXD). The operation parameters were Cu-Kα radiation at a rotating anode generator operated at voltage of 40 kV and at current of 100 mA. The scanning rate was 2°/min at an interval of 0.02°.

2.4.3. TEM characterization

Samples for TEM imaging were sectioned using a Leica Ultracut UCT microtome at 80–100 nm thickness with a diamond knife at −100 °C. The sections were collected from water on 300 mesh carbon-coated copper grids. TEM imaging was done using a JEOL 1200EX electron microscope operating at an accelerating voltage of 100 kV. Images were captured using a charged couple detector camera and viewed using Gatan Digital Micrograph software.

2.5. Crystallization behavior

Nonisothermal crystallization kinetic measurements were carried out with a TA instruments Q10 differential scanning calorimeter (DSC) calibrated with indium. The samples of PP and PP/LDH nanocomposite about 200 μm thick were obtained by hot compression molding, disk-like samples about 5 mg weight were taken for DSC measurements. Samples were heated to 200 °C at a rate of 10 °C/min under a nitrogen atmosphere and held for 5 min to destroy any residual nuclei before cooling at the specified cooling rate (2.5, 5, 10 and 20 °C/min). The exothermal curves of heat flow as a function of temperature were recorded to analyze nonisothermal crystallization process and the crystallinity of the samples was determined from the heat of crystallization.

To support the nonisothermal crystallization events and kinetic results analyzed by DSC thermograms, a very thin section of samples was observed under crossed polarizers with a polarizing LEICA-DMRX optical microscopy (POM). A thin sample sandwiched between two glass cover slips was placed inside the Linkam shearing device (CSS450) and the temperature was raised to 200 °C at the rate of 30 °C/min, kept at that temperature for 5 min to ensure complete melting and then they were cooled to room temperature at a rate of 50 °C/min. The morphological features (optical texture images) were captured in Olympus CCD camera.

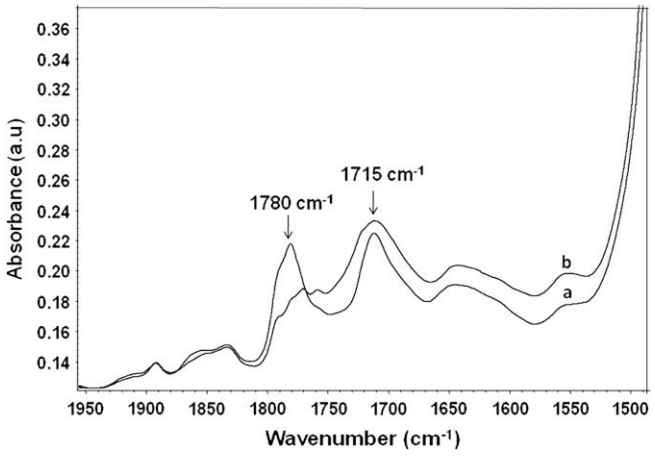

Fig. 2. FTIR spectra of (a) PP and (b) PP/LDH nanocomposite (PPL5).

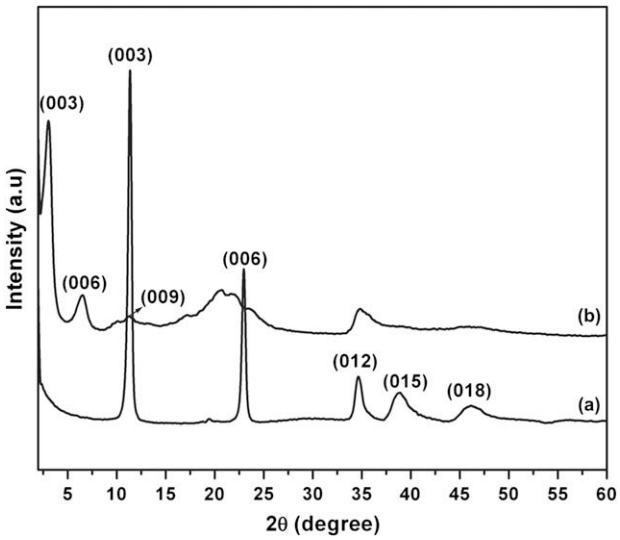

Fig. 3. The X-ray diffraction patterns of (a) Mg_2Al–DDS LDH, (b) Mg_2Al–Cl LDH in the range of $2\theta = 2$–60°.

3. Result and discussion

3.1. Microstructure characterization

3.1.1. FTIR characteristics

It is believed that the maleic anhydride groups can react with the interlayer anionic groups of LDH. Thus, the layered double hydroxides could chemically bind to the macromolecular polypropylene chains, resulting in the prevention of their agglomeration and the break up of large stacking. Such interactions could improve the compatibility between the polymeric matrix and the nanoparticles, increasing the degree of dispersion of the particles, as shown in (Scheme 2). To verify the interactions that take place between the interlayer anions and the maleic anhydride groups of PP-g-MA, FTIR spectroscopy was used. The most characteristic peaks of PP-g-MA, except those of PP, are the two peaks between 1700 and 1800 cm^{-1} (Fig. 2a) corresponding to the anhydride groups. In the spectrum of PP/LDH nanocomposite (Fig. 2b), a strong absorbance at 1780 cm^{-1} has been intensively weakened and new band at 1714 cm^{-1} is observed, maybe due to their reaction with the anhydride groups and this could be of evidence that such reactions take place. This shift is maybe the result of the aforementioned interactions that facilitate polymer chains to intercalate into the lamellas.

3.1.2. XRD characteristics

The XRD patterns in the range of $2\theta = 2°$–60° for Mg_2Al–Cl LDH and Mg_2Al–DDS LDH samples are shown in Fig. 3, where it is seen that these materials are highly crystalline in nature and have layered geometry. The position of the basal peak (003) indicates the interlayer spacing between two metal hydroxide sheets (d_{003}) and was calculated to be 0.76 nm from $2\theta = 11.41°$ for original Mg_2Al–Cl LDH (Fig. 3a), whereas, the basal position peak (003) for organo-modified LDH i.e. Mg_2Al–DDS (Fig. 3b) has been significantly

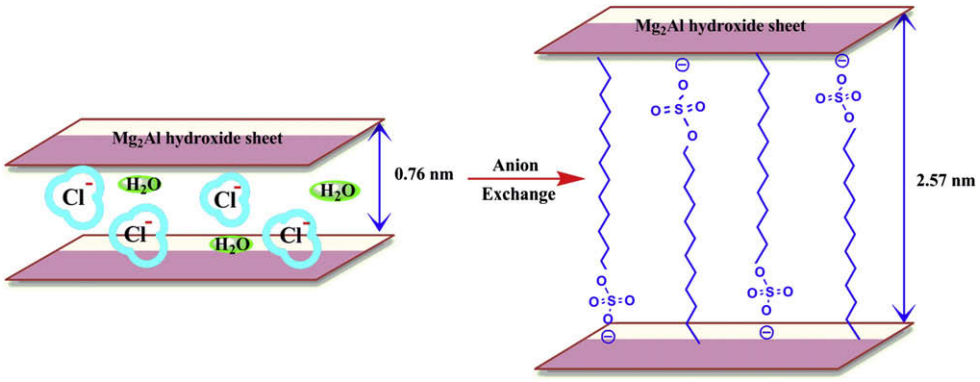

Scheme 1. Schematic diagram of anion exchange in Mg_2Al LDH.

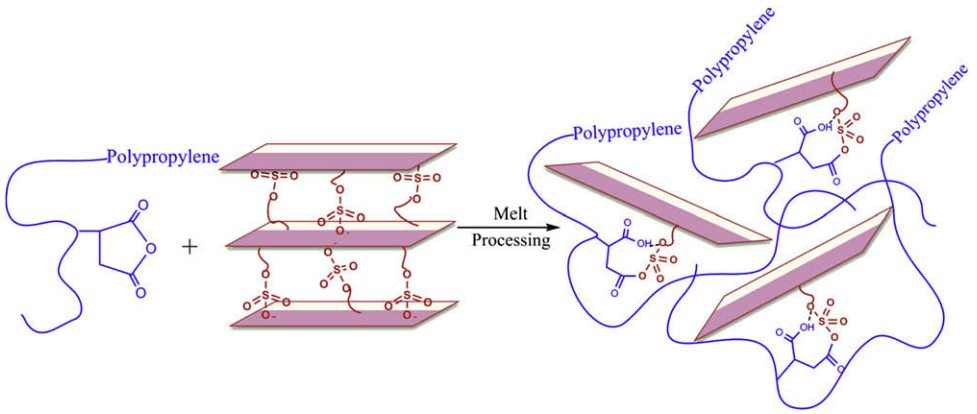

Scheme 2. Conceptual diagram of PP-g-MA/LDH interaction to form the intercalated/exfoliated networks.

shifted towards lower angle, $2\theta = 3.04^\circ$, corresponding to an enlarged interlayer distance from 0.76 nm to 2.57 nm after successive organic modification (Scheme 1). This result indicates that a high degree of anion exchange with dodecyl sulfate was achieved. The intercalation of dodecyl sulfate groups not only enlarges the gallery between the nanolayers, but also improves the interfacial properties between the Mg_2Al–DDS LDH platelets and PP, and thus facilitates the crawling (i.e. intercalation) of PP chains within Mg_2Al–DDS LDH galleries.

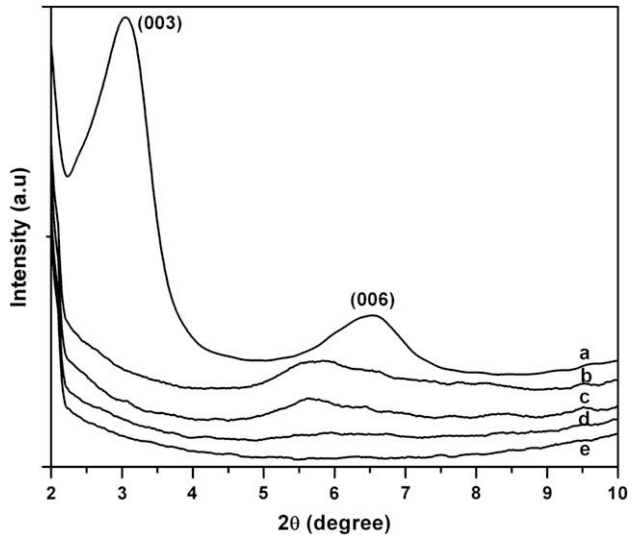

Fig. 4. The X-ray diffraction patterns of (a) Mg_2Al–DDS LDH, (b) PPL5, (c) PPL3, (d) PPL1, and (e) PP in the range of $2\theta = 2$–10°.

In nanocomposites, the extent of intercalation of nanofiller having layered structure was analyzed by XRD. The complete disappearance of XRD peaks may reveal high degree of exfoliation or the presence of small diffracting volume as in the cases of low filler loading. Direct observation by TEM is then necessary to characterize an exfoliation state. Fig. 4(a–d) shows XRD analysis of PP and PP/LDH nanocomposites, a significant change in position of the basal peak was observed. The characteristic crystalline basal position peak of Mg_2Al–DDS LDH at (003) Fig. 4(a) has been completely disappeared in the case of PP/Mg_2Al–DDS LDH nanocomposites Fig. 4(b–d). Moreover, the higher order basal position peak at (006) of PPL3 and PPL5 has been shifted towards lower angle and becomes broader. The overall XRD results suggested that the stacking layers of the Mg_2Al–DDS LDH in these samples were fully/partially separated and an exfoliated/intercalated PP/LDH nanostructure was formed.

3.1.3. TEM characteristics

The microstructure of the nanocomposites was investigated by TEM and micrographs are shown in Fig. 5, they, confirm the fine dispersion of 5 wt% Mg_2Al–DDS LDH in PPL5 sample. The micrograph shows that LDH nanolayers are well dispersed and intercalated throughout the PP matrix (Fig. 5a). Dark lines in the micrograph represent the LDH layers. From the TEM observations at high magnification (Fig. 5b), it is clear that the delamination took place resulting in the presence of single double hydroxide layers as well as tactoids with reduced thickness. These images support XRD analysis shown in Fig. 3.

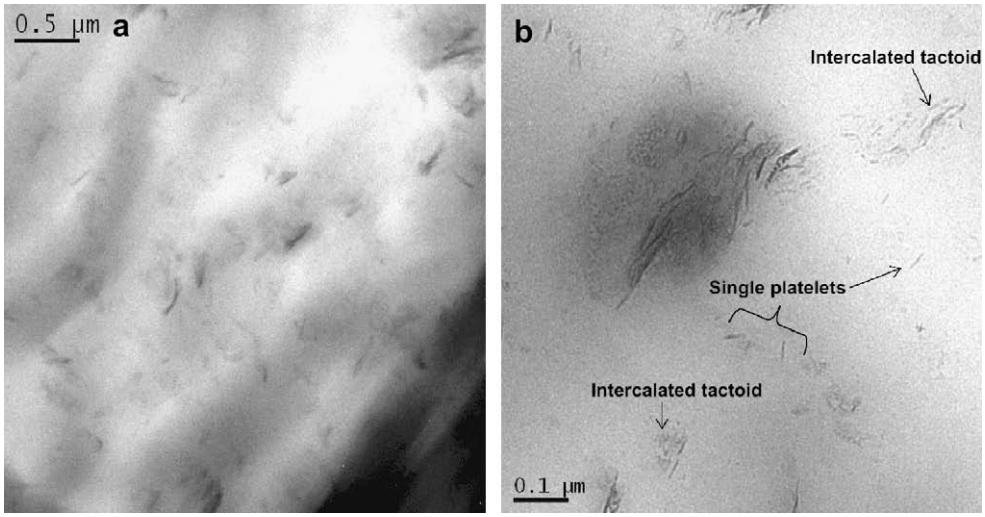

Fig. 5. TEM micrograph of PPL5 (a) 500 nm and (b) 100 nm magnifications.

3.2. Nonisothermal crystallization behavior

The study of nonisothermal crystallization behavior is important because most of the current processing techniques of polymeric materials follow the nonisothermal crystallization process. The crystallization behavior of PP and PP/LDH nanocomposites was studied at cooling rates (α) between 2.5 and 20 °C/min. Fig. 6(a and b) shows typical nonisothermal crystallization thermograms of PP and PP/LDH nanocomposites. From these curves, some useful parameters for the nonisothermal crystallization analysis, such as the onset temperature of crystallization (T_o), the crystallization temperatures, e.g. the exothermic peak maxima (T_p) and the end temperature of crystallization (T_∞) can be obtained. The crystallization temperature (T_p) and the percent crystallinity (X_c) of the PP phase are listed in Table 1. The enthalpy of crystallization (ΔH_c) has also been calculated from the enthalpy of crystallization normalized to the PP content, assuming that the thermodynamic contribution of the LDH phase is negligible. The percent crystallinity (X_c) of pure PP and the PP nanocomposites was determined by Eq. (1), where the value of the heat of crystallinity of pure crystalline PP (ΔH_c^0) was assumed to be 146.5 J/g. [33].

$$X_c = \frac{\Delta H_c}{\Delta H_c^0} \times 100 \tag{1}$$

From DSC thermograms [Fig. 6(a and b) and Table 1] at various cooling rates (2.5, 5, 10 and 20 °C), it is clear that the crystallization peak temperature, for nanocomposites is higher than those of pure PP and decreases with increasing cooling rates. The faster the cooling rate, the lower the temperature range at which the crystallization occurs. At a slower cooling rate, there is sufficient time to activate nuclei; therefore, the crystallization can occur at a higher temperature [20]. For example, the crystallization temperature of PP increased by 15 °C in the presence of LDH nanoparticles whereas decreased when the cooling rate was increased.

The plots, which show the variation of the peak temperature with cooling rates, for the PP/LDH nanocomposites are shown in Fig. 7. It is obvious that the peak temperature at a given cooling rate increases with increasing LDH content, this phenomenon can be explained by the heterogeneous nucleation effect of Mg_2Al–DDS LDH nanoparticles on PP macromolecular segments which can be easily attached to the surface of the Mg_2Al–DDS LDH, which leads to the crystallization of PP to occur at a higher crystallization temperature.

3.3. Nonisothermal crystallization kinetics

In order to further analyze the nonisothermal crystallization process, the crystallization kinetics of PP and PP/LDH nanocomposites is compared. From dynamic crystallization experiments, data form the crystallization exotherms as a function of temperature; dH_c/dT can be obtained, for each cooling rate.

The relative degree of crystallinity as a function of temperature, X_T, can be calculated according to Eq. (2):

$$X_T = \frac{\int_{T_o}^{T} (dH_c/dT)dT}{\int_{T_o}^{T_\infty} (dH_c/dT)dT} \tag{2}$$

where, T_o and T_∞ are the temperatures at which crystallization starts and ends, and dH_c/dT is the heat flow rate. The development of relative degree of crystallinity X_T as a function of temperature, T, for PP and its nanocomposites at various cooling rates is shown in Fig. 8(a). The plots of X_T versus T for PP and PP/LDH nanocomposites are similar and all these curves have the same sigmoidal shape, implying that only a lag effect of cooling rate on crystallization is observed.

In nonisothermal crystallization, the temperature can be related to crystallization time scale by using the following equation:

$$t = \frac{(T_o - T_p)}{\alpha} \tag{3}$$

(where T_o is the onset temperature at a crystallization time $t = 0$, T_p is the temperature at crystallization time t, and α is the cooling rate). The results show that the higher the cooling rate, the shorter the time for completing crystallization. According to Eq. (3) the value of T on the X-axis can be transposed into the crystallization time (t) as shown in Fig. 8(b).

The half crystallization time ($t_{1/2}$) is defined as the half period (i.e. 50% crystallization), from the onset of crystallization and the end of crystallization. The t and $t_{1/2}$ values for PP and its nanocomposites can be obtained from Fig. 9, and the results are listed in Table 2. It is apparent that the value of $t_{1/2}$ decreases with increasing cooling rate. Moreover, at a given cooling rate, the $t_{1/2}$ value for PP/LDH nanocomposites is lower than that for PP and even decreases with increasing LDH content. These results signify that addition of Mg_2Al–DDS LDH particles could act as heterogeneous nucleating agents to facilitate the overall crystallization process. Such a similar trend was observed in the case of PHB/LDH nanocomposite [31].

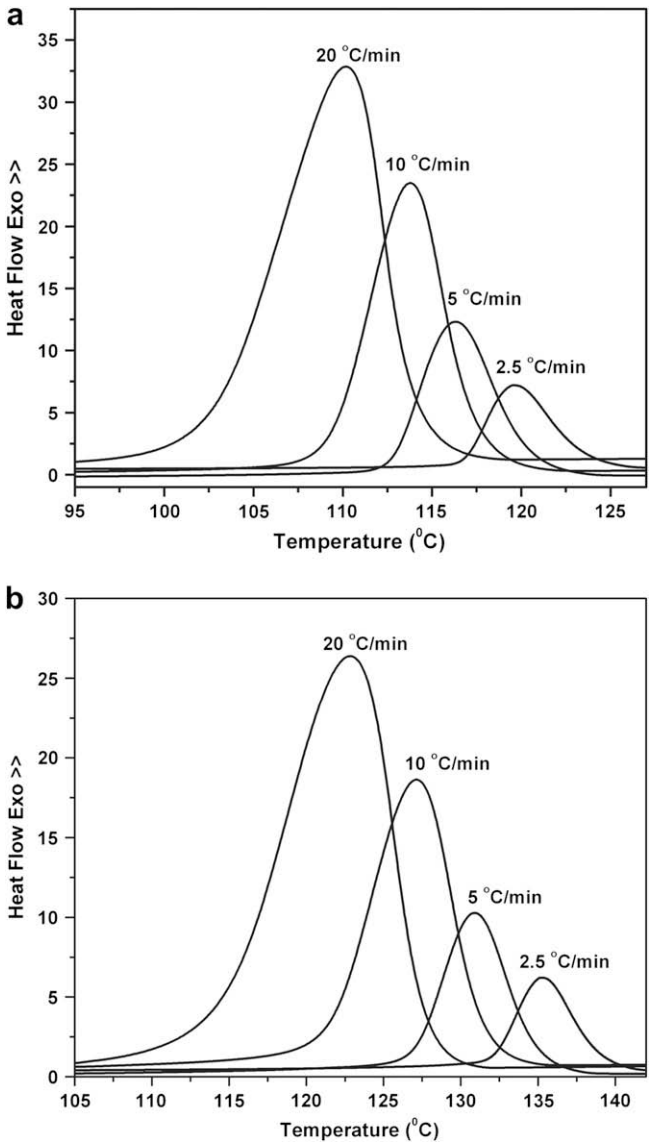

Fig. 6. DSC thermograms of nonisothermal crystallization at different cooling rates: (a) PP and (b) PPL5.

In order to understand fully, the evolution of crystallinity during the nonisothermal crystallization, the Ozawa, the Avrami and the Liu models (modified Avrami–Ozawa method) were employed to analyze the nonisothermal crystallization kinetics of PP and its nanocomposites.

3.3.1. Nonisothermal crystallization kinetics by using the Ozawa model

According to Ozawa theory [34], the nonisothermal crystallization process is a result of infinitesimally small isothermal

Table 1
Crystallization temperature and maximum percent crystallinity of PP/LDH nanocomposites for cooling rates of 2.5, 5, 10 and 20 °C/min.

Sample	2.5 °C/min		5 °C/min		10 °C/min		20 °C/min	
	T_p (°C)	X_c %	T_p (°C)	X_c %	T_p (°C)	X_c %	T_p (°C)	X_c %
PP	119.60	66	116.33	67	113.81	66	110.15	62
PPL1	132.74	63	129.18	64	125.16	66	121.32	67
PPL3	134.44	65	130.75	69	126.85	68	122.85	66
PPL5	135.24	67	131.89	64	128.17	65	123.85	66

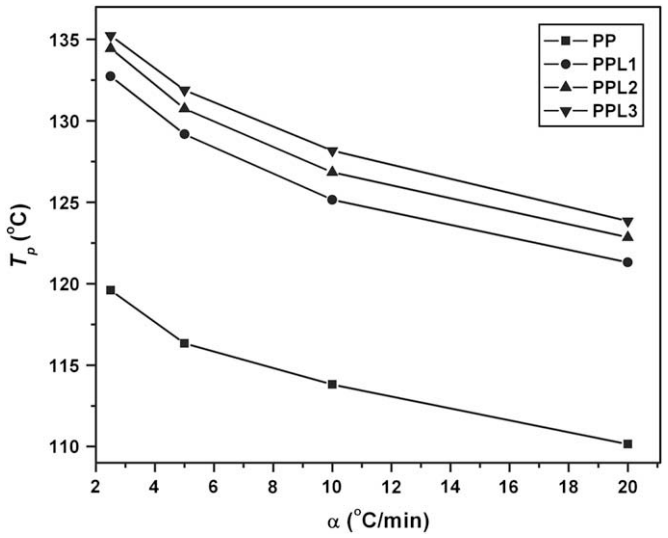

Fig. 7. Crystallization peak temperature versus cooling rate for PP and PP/LDH nanocomposites.

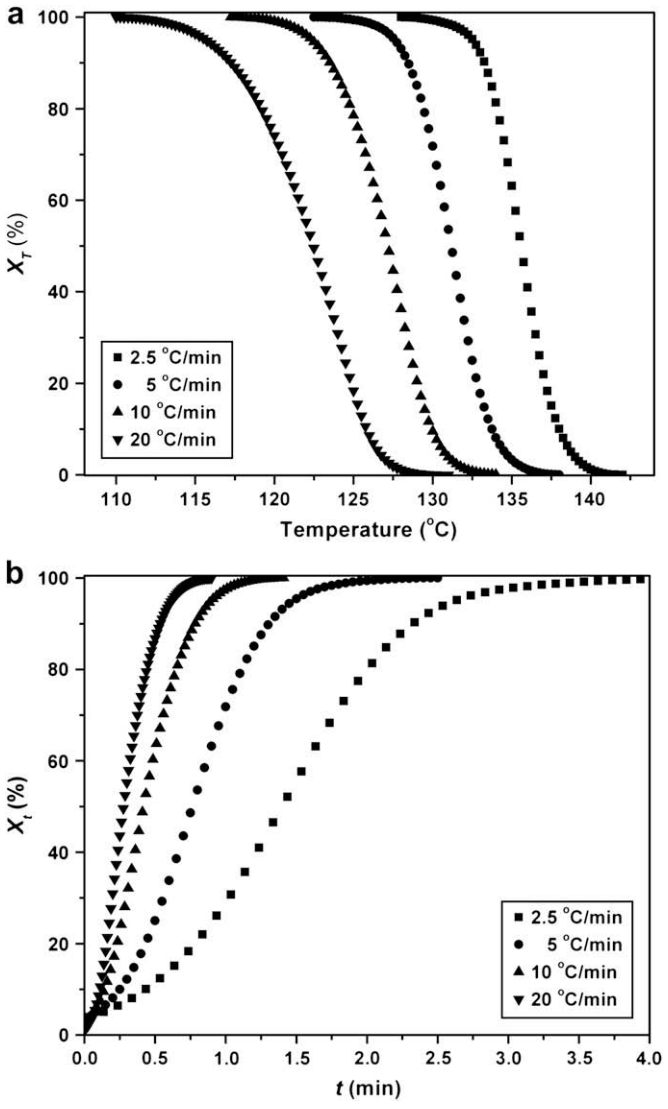

Fig. 8. The relative degree of crystallinity (a) with temperature and (b) with time for the crystallization of PPL5 at different cooling rates.

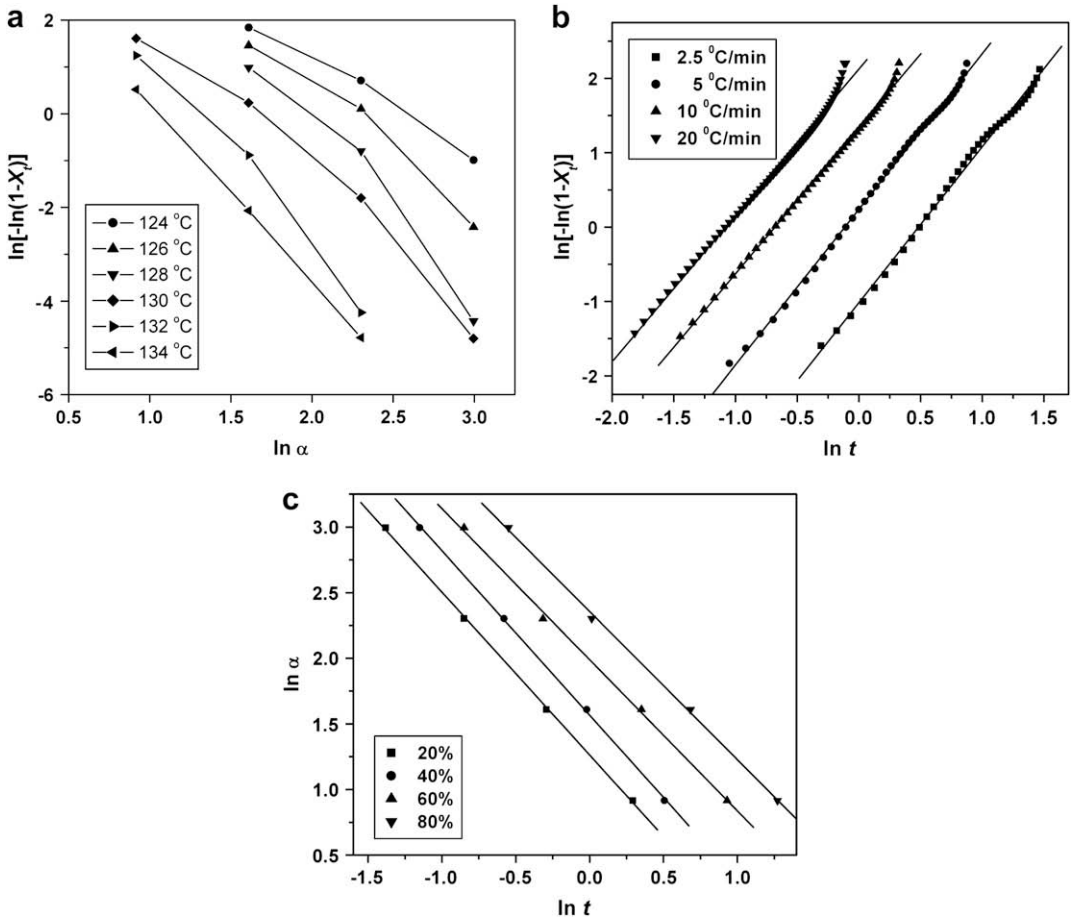

Fig. 9. (a) Ozawa plots of $\ln[-\ln(1-X_t)]$ versus $\ln\alpha$ (b) Avrami plots of $\ln[-\ln(1-X_t)]$ versus $\ln t$ and (c) Liu plots of $\ln\alpha$ versus $\ln t$ during nonisothermal crystallization process of PP/LDH nanocomposite (PPL5).

crystallization steps. According to this model, the degree of conversion at temperature T, X_T, can be written as a function of cooling rate:

$$1 - X_T = \exp(-K(T)/\alpha^m) \tag{4}$$

where $K(T)$ is the function of cooling crystallization, α is the cooling rate and m is the Ozawa exponent that depends on the dimension of crystal growth. The double logarithmic form of Eq. (4) is

$$\ln[-\ln(1-X_T)] = \ln K(T) - m\ln\alpha \tag{5}$$

A plot of $\ln[-\ln(1-X_T)]$ versus $\ln\alpha$ at a given temperature should result in a straight line if the Ozawa method is valid. The kinetic parameters, m and $K(T)$ can be obtained from the slope and the intercept, respectively. Ozawa plots for dynamic crystallization of the PPL5 are shown in Fig. 9(a). The curves in the plot of PP show better linear relationship but PP nanocomposite containing 5% LDH deviates from linearity and an increase in curvature was observed. These results show that PP/OMMt can be analyzed by the Ozawa method which is in agreement with previously reported [35] but the nanocomposite, PP/LDH cannot be fit by Ozawa model. The reason for this difference is that, Ozawa in his approach ignored secondary crystallization, dependence of the fold length on temperature [36] and also the constant value of cooling function over the entire crystallization process [37]. Thus, the Ozawa method was found to be inapplicable for the nonisothermal kinetic modelling of PP/LDH nanocomposites.

3.3.2. Nonisothermal crystallization kinetics by using Avrami model

Generally isothermal crystallization kinetics is explained by Avrami equation [38] but Eq. (6), was also adopted as an alternative approach [39], according to which the equivalent time dependent crystallinity X_t can be expressed as,

$$X_t = 1 - \exp(-Z_t t^n) \tag{6}$$

Table 2
Nonisothermal crystallization parameters T_p, T_o, t and $t_{1/2}$ for PP and its nanocomposites at various cooling rates.

Sample	α (°C/min)	T_p (°C)	t (min)	T_o (°C)	$t_{1/2}$ (min)
PP	2.5	119.60	1.59	123.58	2.10
	5	116.33	0.818	120.42	1.03
	10	113.81	0.359	117.40	0.57
	20	110.15	0.1875	113.92	0.41
PPL1	2.5	132.74	1.7	136.99	1.82
	5	129.18	1.018	134.27	0.89
	10	125.16	0.538	130.54	0.54
	20	121.32	0.237	126.06	0.34
PPL3	2.5	134.44	1.572	138.37	1.55
	5	130.75	0.806	134.78	0.81
	10	126.85	0.424	131.09	0.50
	20	122.85	0.225	127.30	0.33
PPL5	2.5	135.24	1.54	139.09	1.37
	5	131.89	0.602	134.90	0.78
	10	128.17	0.308	131.35	0.48
	20	123.85	0.167	127.59	0.30

Table 3
Nonisothermal crystallization parameters obtained by Avrami and Jeziorny methods.

Sample	α (°C/min)	$\ln Z_t$	Z_c	n
PP	2.5	0.84	2.52	2.82
	5	1.48	2.40	2.62
	10	1.72	1.74	1.92
	20	2.18	1.55	1.62
PPL1	2.5	0.85	2.55	2.81
	5	1.48	2.41	2.09
	10	1.77	1.79	1.87
	20	2.14	1.52	1.62
PPL3	2.5	0.87	2.61	2.85
	5	1.52	2.50	2.28
	10	1.67	1.70	1.93
	20	2.16	1.54	1.70
PPL5	2.5	1.01	2.99	2.95
	5	1.63	2.78	2.95
	10	1.83	1.86	2.06
	20	2.12	1.58	1.96

where X_t is relative degree of crystallinity at crystallization time t, n is the Avrami exponent and Z_t is the crystallization rate constant involving both nucleation and growth rate parameters. As before Eq. (6) can be liberalized in its double logarithmic form to give Eq. (7).

$$\ln[-\ln(1-X_T)] = \ln Z_t + n \ln t \tag{7}$$

By fitting the experimental data to Eq. (7), the values of n and Z_t can be obtained from the slope and intercept of the plots of $\ln[-\ln(1-X_t)]$ versus $\ln t$ for each cooling rate as shown in Fig. 9(b). From the figure, it can be seen that straight lines are obtained in each cooling rate. It should be taken into account that in nonisothermal crystallization, Z_t and n do not have same physical significance as in isothermal crystallization because under nonisothermal crystallization, the temperature changes constantly. Since the rate of nonisothermal crystallization depends on the cooling rate, Jeziorny [40] suggested that the rate parameter Z_t should be corrected for the influence of cooling rate α of the polymer. The parameters characterizing the kinetics of nonisothermal crystallization were given as follows:

$$\ln Z_c = \ln Z_t/\alpha \tag{8}$$

The results obtained from the Avrami plots and the Jeziorny methods are listed in Table 3.

Table 4
Kinetic parameters for the PP and PP–LDH nanocomposites at different relative degrees of crystallinity by Liu method.

Sample	X_t (%)	a	$F(T)$
PP	20	1.08	4.71
	40	1.06	6.55
	60	1.12	8.41
	80	1.19	11.47
PPL1	20	1.10	4.52
	40	1.13	6.11
	60	1.12	8.15
	80	1.17	11.03
PPL3	20	1.12	3.85
	40	1.13	5.63
	60	1.19	6.87
	80	1.23	10.74
PPL5	20	1.12	3.52
	40	1.15	4.75
	60	1.24	7.24
	80	1.25	10.48

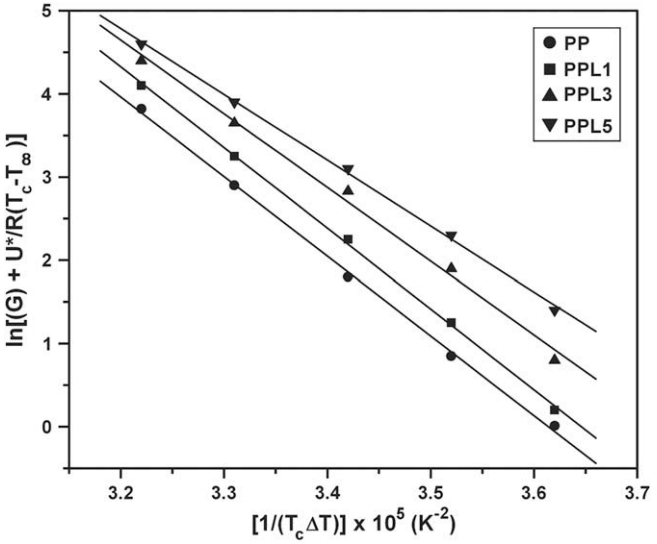

Fig. 10. The plots of $\ln G + U^*/(R(T_c - T_\infty))$ versus $1/(T_c - Tf)$ for PP and PP/LDH nanocomposites.

The Avrami exponent is known to be influenced by the molecular weight, nucleation type, and secondary crystallization, and in general, not much influenced by the temperature. The values of the Avrami exponent for PP–LDH nanocomposites are higher (varied from 1.9 to 2.9) than that for pure PP (varied from 1.6 to 2.8) for given cooling rate, indicating that LDH nanolayers act as nucleating agents and govern a typical heterogeneous nucleation mechanism in the crystallization kinetics of PP–LDH nanocomposites. The Z_c values of the PP–LDH nanocomposites are, as expected, higher than that of the pure PP as the same cooling rate, showing that incorporation of nano LDH could crystallize PP at quicker rate. These results are similar to other 2D reinforcing PP nanocomposites [20,41].

3.3.3. Nonisothermal crystallization kinetics by Liu model (modified Avrami–Ozawa models)

Liu et al. [42] developed a method by combining the Ozawa and Avrami equations to describe the nonisothermal crystallization kinetics which is applicable in many nanocomposite systems [20,43]. Therefore, the corresponding kinetic equation was used here to study the nonisothermal crystallization behavior of the PP–LDH nanocomposites. As the degree of crystallinity was related to the cooling rate α and the crystallization time t (or temperature T), the relation between α and t could be defined for a given degree of crystallinity. Consequently, using Eq. (3) and combining Eqs. (5) and (7) a new kinetic model is derived for nonisothermal crystallization:

$$\ln Z_t + n \ln t = K(T) - m \ln \alpha \tag{9}$$

At given crystallinity X_t, Eq. (9) can be rearranged to

Table 5
Interfacial free energies (σ_e) and kinetic parameter (K_g) under different crystallization processes.

Sample	K_g[a] (10^5 K^2)	σ_e[a] (erg/cm^2)	K_g[b] (10^5 K^2)	σ_e[b] (erg/cm^2)
PP	10.21	125.3	10.18	124.9
PPL1	9.57	108.4	9.61	108.8
PPL3	8.85	94.2	8.87	94.4
PPL5	7.91	87.8	7.86	87.2

[a] Isothermal crystallization.
[b] Isoconversional approach/nonisothermal crystallization.

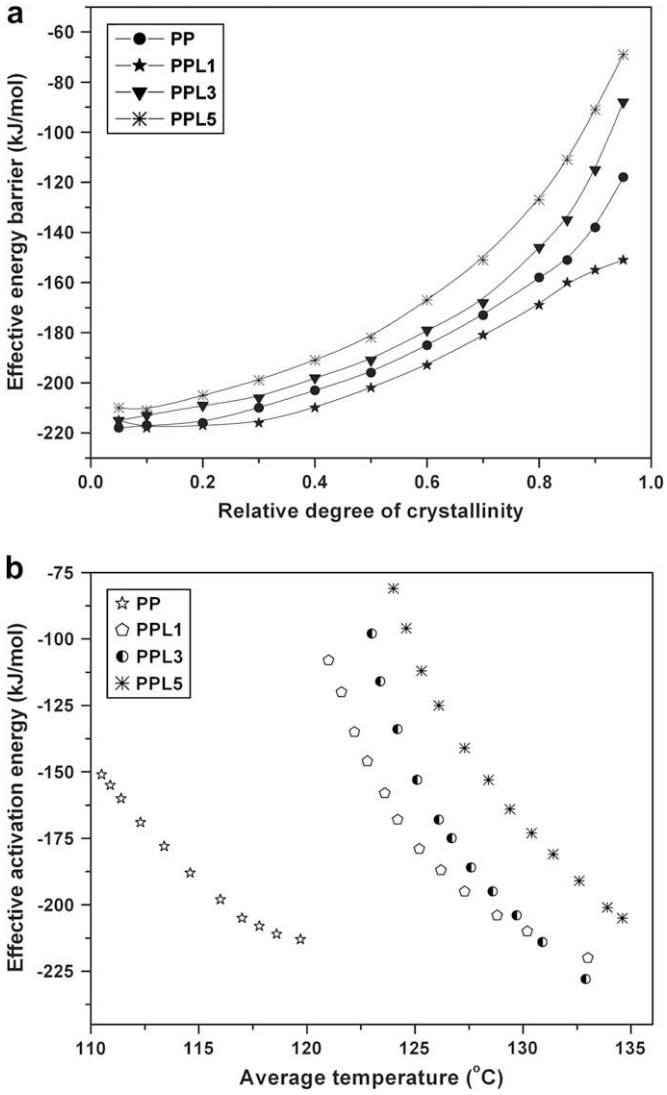

Fig. 11. Dependence of the effective activation energy on the extent of (a) relative crystallization (b) average temperature (isoconversional analysis) for the PP and PP/LDH nanocomposites.

$$\ln \alpha = \ln F(T) - a \ln t \tag{10}$$

where, $F(T) = [K(T)/Z_t]^{1/m}$ refers to the value of cooling rate that must be selected within a unit of crystallization time when the measured systems reach a certain degree of crystallinity; and a is the ratio of Avrami exponent n to Ozawa exponent (m) that is n/m. It can be seen that $F(T)$ has a definite physical and practical meaning. Indeed, according to Eq. (10), at a given degree of crystallinity, plotting $\ln \alpha$ versus $\ln t$ should yield a linear relationship. The kinetic parameters $F(T)$ and α are determined from the intercept and slope of the lines, respectively. Plots of $\ln \alpha$ versus $\ln t$ at various degree of crystallinities for PP and PP/LDH nanocomposites are presented in Fig. 9(c).

From, Fig. 9(c), it can be seen that these plots show good linearity, which verifies the advantage of the combined approach applied in this case. The values for a and $F(T)$ are listed in Table 4. The value of a varies from 1.08 to 1.19 for pure PP and from 1.10 to 1.25 for PP/LDH nanocomposites. Almost all a values of neat PP are lower that those of its nanocomposites at the same relative degree of crystallinity. This phenomenon is similar to the earlier reports of PP/SiO_2 [22], PP/clay [23] and PP/CNT [25]. The values of $F(T)$ systematically increase with increasing relative degree of crystallinity and are lower in the presence of nano-scale reinforcement as reported for other nano-scale reinforcements [22–26] which indicates that PP/LDH nanocomposites crystallize at a faster rate than PP.

3.3.4. Crystal growth and surface free energy

The crystallization thermodynamics and kinetics of the nanocomposites have been analyzed on the basis of the theory of Hoffman–Lauritzen [44,45]. Accordingly, the crystal growth (G), depends on temperature, T, as follows:

$$G = G_0 \exp\left[-\frac{U^*}{R(T_c - T_\infty)}\right] \exp\left[-\frac{K_g}{T_c \Delta T f}\right] \tag{11}$$

$$\ln G + \left[\frac{U^*}{R(T_c - T_\infty)}\right] = \ln G_0 \left[-\frac{K_g}{T_c \Delta T f}\right]$$

where G_0 is the pre-exponential factor, U^* is the activation energy of the segmental jump, the first exponential term contains the contribution of diffusion process to the growth rate, while second exponential term is contribution of the nucleation process; U^* and T_∞ are the Vogel–Fulcher–Tamman–Hesse (VFTH) parameters describing the transport of polymer segments across the liquid/crystal interphase, $\Delta T = T_m - T_c$ the under cooling, $f = 2T_c(T_m + T_c)$ the correction factor. The universal values used for the VFTH parameters are $U^* = 1500$ cal/mol (6300 J/mol) and $T_\infty = (T_g - 30\ \mathrm{K})$ [45] In this study the T_g value of PP used was 270 K [46] and the equilibrium melting temperature T_m was set equal to 212.1 °C. This value found by Marand and coworkers [47] using nonlinear Hoffman–Weeks extrapolation. The kinetic parameter, K_g is the term connected with the energy required for the formation of the nuclei of critical size and can be expressed as:

$$K_g = \frac{nb\sigma\sigma_e T_m}{\Delta h_f k_B} \tag{12}$$

where n is the variable that considers the crystallization regime and assumes the value $n = 4$ for regimes I and III and $n = 2$ for regime II [48]. In the present work, the crystallization is assumed to take place in regime III according to Marand and coworkers. [47], b is the distance between two adjacent fold planes taken as 6.26×10^{-10} m assuming (110) growth front [47], σ and σ_e are the lateral and fold surface free energies, k_B is the Boltzmann constant ($k_B = 1.38 \times 10^{-23}$ J/K), $\Delta h_f = 1.93 \times 10^8$ is the heat of fusion per unit volume of crystal [49]. To verify an isoconversional method for nonisothermal crystallization of PP/LDH nanocomposites, the values of K_g for PP and PP/LDH hybrid composites were obtained from DSC data on isothermal crystallization using Eq. (11), in which the values of G and G_0 were substituted with $(1/t_{1/2})$ and $(1/t_{1/2})_0$, respectively [50]. The plots of $\ln G + U^*/(R(T_c - T_\infty))$ versus $1/(T_c - Tf)$ are shown in Fig. 10 and it shows that the experimental data can be reasonably fitted with straight lines. From the slope the value of K_g can be obtained.

In this article, the values of K_g obtained from Eqs. (9) and (14) were used to estimate the surface free energy (σ_e) and summarized in Table 5. It has been observed that values of σ_e are very close to that obtained by isoconversional method. There is clear tendency for σ_e to decrease as the LDH content is increased. As is well known, a foreign surface frequently reduces the nucleus size needed for crystal growth. The decrease of σ_e could indicate an increase in the entropy of folding and therefore the formation of less homogeneous and regular folding surface. As the composites have a higher melt viscosity than neat PP, the chain movements are restricted during crystallization and will form a less regular folding pattern in the

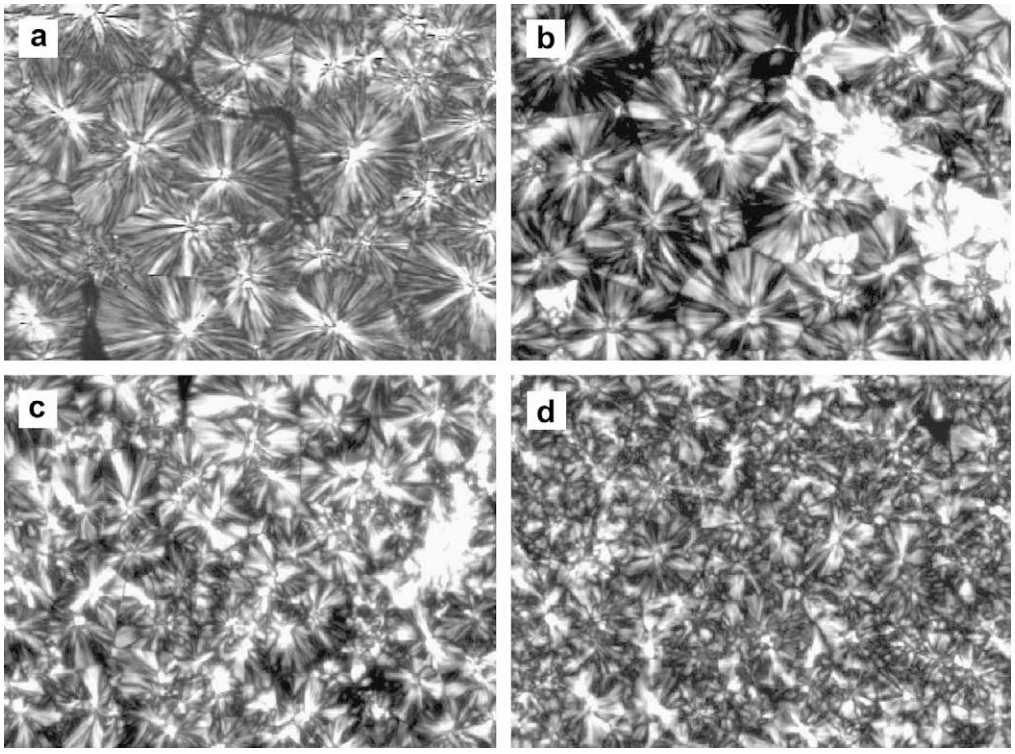

Fig. 12. Optical micrographs of (a) PP and (b) PPL1 (c) PPL3 and (d) PPL5 under a polarizing microscope.

crystals. Based on the results of PP/LDH nanocomposites we conclude that the addition of LDH at nanometric level reduces the creation of new surface, hence leading to faster crystallization rate.

3.3.5. Effective activation energies for nonisothermal crystal growth

As described earlier, the crystallization peak temperature is cooling rate-dependent. For nonisothermal crystallization processes, it is also interesting to evaluate effective activation energy ΔE, several mathematical procedures have been proposed in literature [51,52]. Among them Kissinger method [51] was one of the most popular approach for evaluating effective activation energy of nonisothermal crystallization. However, Vyazovkin and Sbirrazzuoli [53] demonstrated that this method provided invalid results when applied to the processes that occurred on melt crystallization. To this concern, differential isoconversional method of Friedman [54] and Vyazovkin et al. [55] found most appropriate.

The Friedman equation is expressed as:

$$\ln(\mathrm{d}X/\mathrm{d}t)_X = \text{constant} - \frac{\Delta E_X}{RT_X} \tag{13}$$

where, $\mathrm{d}X/\mathrm{d}t$ is the instantaneous crystallization rate as a function of time at a given conversion X. According to this method, the X_t function obtained from the integration of the experimentally measured crystallization rates is initially differentiated with respect to time to obtain the instantaneous crystallization rate, $\mathrm{d}X/\mathrm{d}t$ Furthermore, by selecting appropriate degrees of crystallinity (i.e. from 2 to 98%) the values of $\mathrm{d}X/\mathrm{d}t$ at a specific X are correlated to the corresponding crystallization temperature at this X, i.e. T_x. Then, by plotting the left hand side of Eq. (13) with respect to $1/T_x$ a straight line must be obtained with a slope equal to $\Delta E_x/R$. Plots of $\ln(\mathrm{d}X/\mathrm{d}t)$ versus $1/T_x$ at different relative crystallinity are obtained as a straight lines, permitting thus the calculation of the effective energy barrier at different degrees of crystallinity. The correlation coefficient obtained was always greater than 0.980.

The dependence of the effective activation energy on the context of relative crystallization of the PP and PP/LDH nanocomposites is presented in Fig. 11(a). As it can be seen, ΔE is strongly dependent on the LDH content and increases with the increase in relative degree of crystallinity for all nanocomposites and neat PP at $X > 20\%$. In all the cases, ΔE takes great negative values at lower extent of conversion that corresponds to temperature closer to the melting point. For the nanocomposites, it is observed that 1% LDH show lower values of ΔE and then increases with increasing LDH content. These results indicate that the addition of 1% LDH in to PP causes more heterogeneous nucleation (lower ΔE). The addition of more LDH expected to cause more heterogeneous nucleation, but higher the content of LDH also reduces transportation ability of polymer chains and prevents the PP macromolecule segment from rearranging, and as a result, increases the ΔE during crystallization process. Accordingly, the addition of LDH may accelerate the overall nonisothermal crystallization process of PP.

Furthermore, according to recent reports, the effective activation energy barrier can be plotted as a function of temperature by taking an average temperature associated with certain α value shown in Fig. 11(b). It is can be seen, again at given crystallization temperature, the 1% LDH nanocomposite exhibits lower value of the effective activation energy while the 5% LDH shows higher ΔE. The values of ΔE were negative, indicating that the rate of crystallization increased with decreasing temperatures. The absolute value of ΔE for 5% nanocomposites was higher than that of PP, which revealed that polypropylene segments require more energy to rearrange in presence of LDH, since LDH nanolayers might hinder the mobility of chain segments. These plots also can be used in evaluating Lauritzen–Hoffman parameters, K_g and U^*. The temperature dependence of the effective activation energy is defined as:

$$E_\alpha(T) = U^* \frac{T^2}{(T - T_\infty)^2} + K_g R \frac{T_m^2 - T^2 - T_m T}{(T_m - T)^2 T} \tag{14}$$

By performing the nonlinear curve fitting based on Levenberg–Marquardt method to the experimental data, the parameter K_g can be evaluated. The estimated values of K_g are listed in Table 5 and found linearly decrease with LDH %. The values of K_g are found to be close to those reported for isothermal crystallization and are used for the determination of surface free energy by using Eq. (12). Herewith, isoconversional method has been successfully employed for non-isothermal crystallization behavior of PP/LDH nanocomposites.

3.4. Spherulitic growth behavior

Fig. 12, shows the POM photographs of the PP and its nanocomposites. The PP, Fig. 12(a) revealed the typical spherulitic structure. Apparently, the spherulite size gradually decreases and gets distorted with the increasing content of LDH [Fig. 12(b–d)]. This phenomenon is attributed to the nucleation effect of the dispersed layered double hydroxide, which provides much more heterogeneous nuclei and reduces the size of spherulite. Because of the colliding and impacting effect, the perfect spherulites could not form when the LDH content was high and the growth of the PP spherulites is restricted. For example, the nucleation of the PPL5 resulted in a large number of nucleus, and caused a large number of spherulites in the limited space that constrain the diffusing motions and conformational transitions of the molecules during crystal growing step, which caused more defects in crystals and diminished the spherulite size [56]. These results were in good agreement with the nonisothermal crystallization behavior observed from DSC thermograms.

4. Conclusions

In conclusion, we have successfully prepared polypropylene/organo-modified layered double hydroxide (LDH) hybrid nanocomposites by direct melt intercalation using PP-g-MA as a compatibilizing agent and the conventional twin-screw extrusion compounding process. The addition of PP-g-MA as a compatibilizer results in a higher adhesion between the PP matrix and LDH nanolayers, due to the interactions that take place between the reactive groups. LDH layers were found to be dispersed at the nanometer level, X-ray diffraction and TEM examinations provided direct evidence for the formation of intercalated and exfoliated nanocomposites.

In nonisothermal crystallization kinetics, it was found that Ozawa model was rather inapplicable, probably due to the inaccurate assumption in the approach regarding secondary crystallization. In contrast, the Avrami plots showed good linearity and were able to explain crystallization kinetics for these systems. The Avrami analysis modified by Jeziorny successfully describes the non-isothermal crystallization process of PP/LDH nanocomposite, together with analysis of Liu et al. The isoconversional analysis was successfully employed to determine the effective energy barrier for nonisothermal crystallization. It was found to vary with conversion and altered by LDH addition. In addition, in the analysis of the activation energy of crystallization, it was shown that the fold surface free energy σ_e of PP chains decreased with increasing LDH content. Different kinetic parameters determined from these models proved that in the nanocomposites, LDH was efficient to start crystallization earlier by nucleation but crystal growth decreased in nanocomposites due to intercalation of polymer chains in the galleries. POM observations also support the DSC results. Consequently, these analyses showed that the addition of a small amount of LDH enhances the PP nucleation mechanism but also hinders the crystallite growth. Finally, it can be concluded that the type of nucleation, growth and geometry of PP crystals markedly change in the presence of nano-sized LDH nanoparticles. It is our belief that such shifts in the mechanism of crystal nucleation and growth leading to the development of a fine grain micron-sized structure for the PP/LDH composites should improve the overall physical properties of the material that are now under investigation.

Acknowledgements

S.P. Lonkar is thankful to Council of Scientific and Industrial Research (CSIR), New Delhi, India, for granting senior research fellowship and also grateful to French Embassy in India for award of Sandwich Ph.D fellowship.

References

[1] Giannelis EP. Appl Organomet Chem 1998;12:675.
[2] Alexandre M, Dubois P. Mater Sci Eng 2000;28:1.
[3] Ray SS, Okamoto M. Prog Polym Sci 2003;28:1539.
[4] Rives V. Layered double hydroxides: present and future. New York: Nova Publishers; 2001.
[5] Costa FR, Saphiannikova M, Wangenknechat U, Henrich G. Adv Polym Sci 2007;270:101.
[6] Meyn M, Beneke K, Lagaly G. Inorg Chem 1990;29:5210.
[7] Leroux F. J Nanosci Nanotech 2006;6:303.
[8] Chen W, Qu B, Ding P. Prog Nat Sci 2006;16:573.
[9] Leroux F, Besse JP. Chem Mater 2001;13:3507.
[10] Costa Fr, Abdel-Goad G, Wangenknechat U, Heinrich G. Polymer 2005;46:4447.
[11] Zammarano M, Bellayer S, Gilman JW, Franceschi M, Beyer FL, Harris RH, et al. Polymer 2006;47:652.
[12] Zammarano M, Franceschi M, Bellayer S, Gilman JW, Meriani S. Polymer 2005;46:9314.
[13] Leroux F, Meddar L, Mailhot B, Morlat-Therias S, Gardette J-L. Polymer 2005;46:3571.
[14] Lee WD, Im SS, Lim HM, Kim KJ. Polymer 2006;47:1364.
[15] Wang GA, Wang CC, Chen CY. Polymer 2005;46:5065.
[16] Günter R, Strobl GR. Progress in understanding of polymer crystallization series: lecture notes in physics. Berlin: Springer-Verlag; 2007. p. 714.
[17] Mandelkern L. Crystallization of polymers. New York: McGraw-Hill; 1964.
[18] Wunderlich B. Macromolecular physics. New York: Academic Press; 1973.
[19] Lorenzo MLD, Silvestre C. Prog Polym Sci 1999;24:917.
[20] Xu WB, Ge ML, He PS. J Polym Sci Part B Polym Phys 2002;40:408.
[21] Maiti P, Nam PH, Okamoto M, Hasegawa N, Usuki A. Macromolecules 2002;35:2042.
[22] Qian J, He P, Nie K. J Appl Polym Sci 2004;91:1013.
[23] He JD, Cheung MK, Yang MS, Qi Z. J Appl Polym Sci 2003;89:3404.
[24] Mucha M, Marszalek J, Fifrych A. Polymer 2000;41:4137.
[25] Grady BP, Pompeo F, Shambaugh RL, Reasasco DE. J Phys Chem B 2002;106:5852.
[26] Page DJYS, Gopakumar TG. Polym J 2006;38:920.
[27] Chen JH, Yao BX, Su WB, Yang YB. Polymer 2007;48:1756.
[28] Chen W, Qu B. Chem Mater 2003;15:3208.
[29] Du L, Qu B, Meng Y, Zhu Q. Compos Sci Technol 2006;66:913.
[30] Hsu SF, Wu TM, Liao CS. J Polym Sci Part B Polym Phys 2006;44:3337.
[31] Hsu SF, Wu TM, Liao CS. J Polym Sci Part B Polym Phys 2007;45:995.
[32] Bandyopadhyay J, Ray SS, Bousmina M. J Nanosci Nanotech 2008;8:1812.
[33] Eder M, Wlochowicz A. Polymer 1983;24:1593.
[34] Ozawa T. Polymer 1971;12:150.
[35] Xu W, Liang G, Wang W, Tang S, He P, Pan WP. J Appl Polym Sci 2003;88:3093.
[36] Addonizio ML, Martuscelli E, Silvestre C. Polymer 1987;28:183.
[37] Joshi M, Butola BS. Polymer 2005;451:4953.
[38] Avrami M. J Chem Phys 1940;8:212.
[39] Chen GX, Yoon JS. J Polym Sci Part B Polym Phys 2005;43:817.
[40] Jeziorny A. Polymer 1978;19:1142.
[41] Yuan Q, Awate S, Misra RDK. Eur Polym J 2006;42:1994.
[42] Liu T, Mo Z, Wang S, Zhang H. Polym Eng Sci 1997;37:568.
[43] Nandi S, Ghosh AK. J Polym Res 2007;14:387.
[44] Lauritzen JL, Hoffman JD. J Appl Phys 1973;44:4340.
[45] Hoffman JD, Miller RL. Polymer 1997;38:3151.
[46] Advance thermal analysis system (ATHAS databank). Available from: http://web.utk.edu/athas/edu.
[47] Xu J, Srinivar S, Marand H, Agarwal P. Macromolecules 1998;31:8230.
[48] Clark EJ, Hoffman JD. Macromolecules 1984;17:878.
[49] Bu HS, Cheng SZD, Wundlich B. Macromol Rapid Commun 1988;9:76.
[50] Lu X, Hay JN. Polymer 2001;42:9423.
[51] Kissinger HE. J Res Natl Bur Stand 1956;57:217.
[52] Takhor RL. Advances in nucleation and crystallization of glasses. Columbus, OH: Americal Chemical Society; 1971. p. 166.
[53] Vyazovkin S, Sbirrazzuoli N. Macromol Chem Phys 2006;206:1511.
[54] Friedman H. J Polym Sci Part C Polym Lett 1964:183.
[55] Vyazovkin S, Sbirrazzuoli N. Macromol Rapid Commun 2004;25:733.
[56] Jiang S, Ji X, An L, Jiang B. Polymer 2001;42:3901.